

Phase-dependent optical response properties in an optomechanical system by coherently driving the mechanical resonator

W. Z. Jia,^{1,*} L. F. Wei,^{1,2} Yong Li,^{3,4} and Yu-xi Liu^{5,6,†}

¹*Quantum Optoelectronics Laboratory, School of Physical Science and Technology, Southwest Jiaotong University, Chengdu 610031, China*

²*State Key Laboratory of Optoelectronic Materials and Technologies, School of Physics Science and Engineering, Sun Yet-sen University, Guangzhou 510275, China*

³*Beijing Computational Science Research Center, Beijing 100084, China*

⁴*Synergetic Innovation Center of Quantum Information and Quantum Physics, University of Science and Technology of China, Hefei, Anhui 230026, China*

⁵*Institute of Microelectronics, Tsinghua University, Beijing 100084, China*

⁶*Tsinghua National Laboratory for Information Science and Technology (TNList), Beijing 100084, China*

(Received 19 August 2014; published 29 April 2015)

We explore theoretically the optical response properties in an optomechanical system under an electromagnetically induced transparency condition but with the mechanical resonator being driven by an additional coherent field. In this configuration, more complex quantum coherent and interference phenomena occur. In particular, we find that the probe transmission spectra depend on the total phase of the applied fields. Our study also provides an efficient way to control propagation of a probe field from perfect absorption to remarkable amplification.

DOI: [10.1103/PhysRevA.91.043843](https://doi.org/10.1103/PhysRevA.91.043843)

PACS number(s): 42.50.Gy, 07.10.Cm, 42.50.Wk

I. INTRODUCTION

Optomechanical systems couple photons and phonons via radiation pressure. Significant research interest in this frontier of optomechanics is motivated by its potential applications in ultrasensitive measurements, quantum information processing, and implementation of novel quantum phenomena at macroscopic scales [1–4]. Recently, a phenomenon resembling electromagnetically induced transparency (EIT) [5–7] in atomic physics, called optomechanically induced transparency (OMIT), is studied theoretically [8–10] and observed experimentally [11–14]. OMIT can be used for slowing and switching probe signals [15] and may be further used for on-chip storage of light pulses via microfabricated optomechanical arrays [16]. OMIT in the nonlinear quantum regime has also been investigated [17–20]. On the other hand, the optomechanically induced absorption (OMIA) phenomenon, which is an analog of electromagnetically induced absorption (EIA) investigated in atomic gas [21,22] and superconducting artificial atoms [23], can also be realized in the optomechanical setup [13,24,25]. And OMIA is a phenomenon closely related to optomechanically induced amplification [13,14,26–28].

To obtain optomechanical analogs of atomic-coherence-related phenomena such as EIT and EIA, the key point is that a mechanical coherence (similar to atomic coherence) must be induced. Specifically, in standard OMIT [8–14] and OMIA [13,24], the coherent oscillation of the mechanical resonator results from a time-varying radiation pressure force induced by the beat of the probe and the control laser. The oscillating mechanical resonator together with the (red- or blue-detuned) control field can further induce sidebands on the cavity field. The generated field with probe frequency can interfere with the original probe field, leading to OMIT or OMIA absorption spectra. On the other hand, in three-level atomic physics, the

atomic coherences can be produced by the direct drive at the microwave frequency [29–31] or by the spontaneously generated coherence [32]. Usually, these additional drives can generate a closed transition loop. These so-called phaseonium systems [33,34] can lead to many remarkable phase-dependent effects such as correlated lasing [35,36] and inversionless gain [29,30,37]. Similarly, in the optomechanical system, one can expect that this type of mechanical coherence can also be generated by directly driving the mechanical resonator, and further used to coherent control the propagation of probe fields. Thus, in this paper, we study the influence of directly produced mechanical coherence on optical response properties of an optomechanical system.

In our study, besides a red-detuned control field and a nearly resonant probe field applied to pump the optical cavity, an additional weak driving field is used to directly excite the mechanical resonator to produce mechanical coherence. In contrast to the strong magnetic driving used for the coherent connection between two electric-dipole-forbidden atomic energy levels [29–31], the weak electric driving is enough for our study here, because there is no selection rule in our system. In this case, the optomechanical cavity can be resonantly excited by directly absorbing a probe photon, or through the phonon-photon process. For the interference effects of these two possible transition paths, the optical response properties for the probe field become phase sensitive, and more complex quantum interference and quantum-coherence-related phenomena will appear. Specifically, gain without inversion (GWI)-like, OMIA and EIT-type spectra can be obtained, depending on the amplitude and phase of the control field. In addition, by adjusting the control field and the additional driving field applied on the mechanical resonator, the probe field can be efficiently manipulated from perfect absorption to remarkable amplification.

The paper is organized as follows. In Sec. II, we introduce the theoretical model for describing the driven optomechanical system. Then, in Sec. III, we study the phase-dependent optical response for the probe field in detail, including

*wenzjia@home.swjtu.edu.cn

†yuxiliu@mail.tsinghua.edu.cn

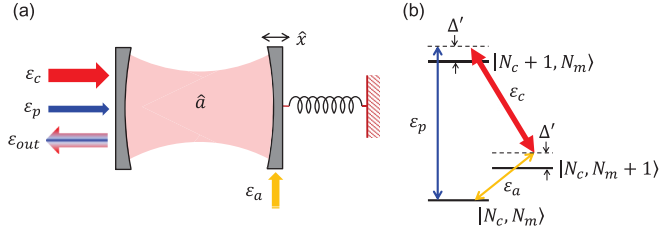


FIG. 1. (Color online) (a) Standard optomechanical setup driven by a control laser and a probe laser, with an auxiliary driving field applied to the mechanical resonator. (b) A block of three energy levels in the system. N_c (N_m) denotes the number of photons (phonons). The control laser with amplitude ε_c resonantly couples the transition $|N_c, N_m + 1\rangle \leftrightarrow |N_c + 1, N_m\rangle$, the probe laser with amplitude ε_p and detuning Δ' couples the transition $|N_c, N_m\rangle \leftrightarrow |N_c + 1, N_m\rangle$, and the auxiliary driving field with amplitude ε_a and detuning Δ' couples the transition $|N_c, N_m\rangle \leftrightarrow |N_c, N_m + 1\rangle$.

GWI-like spectra in Sec. III A, OMIA and EIT-like spectra in Sec. III B, amplification and perfect absorption in Sec. III C, and numerical simulation in Sec. III D. Finally, further discussions and conclusions are given in Sec. IV.

II. THE MODEL

We consider a standard optomechanical system schematically illustrated in Fig. 1(a). The cavity is driven by a strong control laser and a weak probe one, where ω_c (ω_p) and ε_c (ε_p) are the control (probe) laser frequency and amplitude, respectively. Meanwhile, a weak coherent driving field with frequency ω_a and amplitude ε_a is applied to excite the mechanical resonator. Experimentally, a micro- or nanoscale mechanical resonator can be driven by microwave electrical signals [38–40]. For example, in a recent experiment [38], the mechanical element is a thin film of piezoelectric materials AlN, which is sandwiched between two aluminium metal electrodes, enabling strong electromechanical coupling through the piezoelectric effect. We also assume that the frequencies of the three coherent driving fields satisfy the condition $\omega_p - \omega_c = \omega_a$. Figure 1(b) shows a block of three energy levels in the system. Clearly, the three couplings create a set of Δ -type transitions analogous to those in microwave-driving natural atoms [29–31,41], superconducting artificial atoms [42–45], or chiral molecules [46,47]. Thus one can expect that, similar to these quantum systems with closed-loop transition structure, the optical properties of the optomechanical system considered here will be sensitive to the relative phases of three applied fields.

In a frame rotating at the frequency of the coupling field ω_c , The Hamiltonian of the system is of the form,

$$\hat{H} = \hbar\Delta_0\hat{c}^\dagger\hat{c} + \hbar\omega_m\hat{b}^\dagger\hat{b} - \hbar g_0\hat{c}^\dagger\hat{c}(\hat{b}^\dagger + \hat{b}) + \hat{H}_{\text{dr}}, \quad (1)$$

where \hat{c} (\hat{b}) is the photon (phonon) annihilation operator, ω_m is the mechanical resonance frequency, $\Delta_0 = \omega_0 - \omega_c$ is the detuning of the control laser from the bare cavity frequency ω_0 , g_0 is the single-photon coupling strength of the radiation pressure between the cavity field and the mechanical resonator, and \hat{H}_{dr} describes the interaction between the optomechanical

system and the three driving fields:

$$\hat{H}_{\text{dr}} = i\hbar(\varepsilon_c + \varepsilon_p e^{-i\omega_a t})\hat{c}^\dagger + i\hbar\varepsilon_a e^{-i\omega_a t}\hat{b}^\dagger + \text{H.c.} \quad (2)$$

The nonlinear quantum Langevin equations for the operators of the optical and mechanical modes are given by

$$\dot{\hat{c}} = -\left(i\Delta_0 + \frac{\kappa}{2}\right)\hat{c} + ig_0\hat{c}(\hat{b}^\dagger + \hat{b}) + \varepsilon_c + \varepsilon_p e^{-i\omega_a t} + \hat{f}, \quad (3)$$

$$\dot{\hat{b}} = -\left(i\omega_m + \frac{\gamma_m}{2}\right)\hat{b} + ig_0\hat{c}^\dagger\hat{c} + \varepsilon_a e^{-i\omega_a t} + \hat{\xi}. \quad (4)$$

κ and γ_m are the decay rates of cavity and mechanical resonator, respectively. \hat{f} and $\hat{\xi}$ are the quantum and thermal noise operators, respectively. We assume that they satisfy the condition $\langle\hat{f}\rangle = \langle\hat{\xi}\rangle = 0$.

It is not easy to obtain the solutions of the nonlinear Eqs. (3) and (4). However, we are only interested in the linear response of the driven optomechanical system to the weak probe field. Thus, in the case of $|\varepsilon_p|, |\varepsilon_a| \ll |\varepsilon_c|$, we can linearize the dynamical equations of the driven optomechanical system by assuming $\hat{c} = c_s + \delta\hat{c}$ and $\hat{b} = b_s + \delta\hat{b}$. Here c_s and b_s are steady-state values of the system when only the strong driving field is applied. They can be gotten from Eqs. (3) and (4) by assuming $\varepsilon_p, \varepsilon_a \rightarrow 0$ and all time derivatives vanish:

$$c_s = \frac{\varepsilon_c}{i\Delta + \frac{\kappa}{2}}, \quad b_s = \frac{ig_0|c_s|^2}{i\omega_m + \frac{\gamma_m}{2}}, \quad (5)$$

where $\Delta = \Delta_0 - g_0(b_s + b_s^*)$ denotes the effective detuning between the cavity field and the control field, including the frequency shift caused by the mechanical motion. After plugging the ansatz $\hat{c} = c_s + \delta\hat{c}$, $\hat{b} = b_s + \delta\hat{b}$ into Eqs. (3) and (4), and dropping the small nonlinear terms, we can get the linearized quantum Langevin equations for the operators $\delta\hat{c}$ and $\delta\hat{b}$:

$$\delta\dot{\hat{c}} = -\left(i\Delta + \frac{\kappa}{2}\right)\delta\hat{c} + iG\delta\hat{b}^\dagger + \delta\hat{b} + \varepsilon_p e^{-i\omega_a t} + \hat{f}, \quad (6)$$

$$\delta\dot{\hat{b}} = -\left(i\omega_m + \frac{\gamma_m}{2}\right)\delta\hat{b} + i(G\delta\hat{c}^\dagger + G^*\delta\hat{c}) + \varepsilon_a e^{-i\omega_a t} + \hat{\xi}, \quad (7)$$

where $G = g_0 c_s$ is the total (linearized optomechanical) coupling strength.

Now we move into another interaction picture by introducing $\delta\hat{c} \rightarrow \delta\hat{c}e^{-i\omega_a t}$, $\delta\hat{b} \rightarrow \delta\hat{b}e^{-i\omega_a t}$, $\hat{f} \rightarrow \hat{f}e^{-i\omega_a t}$, $\hat{\xi} \rightarrow \hat{\xi}e^{-i\omega_a t}$. In addition, we assume the cavity is driven by a control field at the mechanical red sideband with $\Delta = \omega_m$, the system is operating in the resolved sideband regime $\omega_m/\kappa \gg 1$, the mechanical resonator has a high mechanical quality factor $\omega_m/\gamma_m \gg 1$, and the mechanical frequency ω_m is much larger than $|G|$ and $|\omega_a - \omega_m|$. In this parameter regime, analogous to the rotating wave approximation presented in the context of atomic EIT, one can ignore the fast oscillating terms $e^{2i\omega_a t}$ and get the following equations:

$$\delta\dot{\hat{c}} = \left(i\Delta' - \frac{\kappa}{2}\right)\delta\hat{c} + iG\delta\hat{b} + \varepsilon_p + \hat{f}, \quad (8)$$

$$\delta\dot{\hat{b}} = \left(i\Delta' - \frac{\gamma_m}{2}\right)\delta\hat{b} + iG^*\delta\hat{c} + \varepsilon_a + \hat{\xi}, \quad (9)$$

with $\Delta' = \omega_a - \omega_m = \omega_p - \omega_c - \omega_m$. Then we take the expectation values of the operators in Eqs. (8) and (9). Note that the mean values of the quantum and thermal noise terms are zero (i.e., $\langle \hat{f} \rangle = \langle \hat{\xi} \rangle = 0$). Under steady-state condition $\langle \delta \hat{c} \rangle = \langle \delta \hat{b} \rangle = 0$, one has

$$0 = \left(i\Delta' - \frac{\kappa}{2} \right) \langle \delta \hat{c} \rangle + iG \langle \delta \hat{b} \rangle + \varepsilon_p, \quad (10)$$

$$0 = \left(i\Delta' - \frac{\gamma_m}{2} \right) \langle \delta \hat{b} \rangle + iG^* \langle \delta \hat{c} \rangle + \varepsilon_a. \quad (11)$$

Thus, the expectation value of the operator $\delta \hat{c}$ corresponding to the intracavity field oscillating at the probe frequency reads

$$\langle \delta \hat{c} \rangle = e^{i\phi_p} \left[\frac{\left(\frac{\gamma_m}{2} - i\Delta' \right) |\varepsilon_p|}{\left(\frac{\kappa}{2} - i\Delta' \right) \left(\frac{\gamma_m}{2} - i\Delta' \right) + |G|^2} + \frac{|\varepsilon_a| |G| e^{i\Phi}}{\left(\frac{\kappa}{2} - i\Delta' \right) \left(\frac{\gamma_m}{2} - i\Delta' \right) + |G|^2} \right]. \quad (12)$$

Here the total phase Φ is defined as $\arctan\left(\frac{\kappa}{2\omega_m}\right) + \phi_c + \phi_a - \phi_p$, and ϕ_i is the phase of amplitude ε_i ($i = c, a, p$). In the resolved sideband limit, $\Phi \simeq \phi_c + \phi_a - \phi_p$. In Eq. (12), the first term is the contribution from the usual OMIT effect [8,11], and the second term is the contribution from the phonon-photon parametric process involving the driving on the mechanical resonator. The intracavity field with probe frequency is determined by the interference of these two terms and is strongly dependent on the relative phase of the applied driving fields. Thus we can control the transmission of the probe field by adjusting the total phase Φ .

The output field of the cavity can be derived by the input-output relation [48],

$$\langle \hat{c}_{\text{out}} \rangle + \varepsilon_c + \varepsilon_p e^{-i(\omega_p - \omega_c)t} = \kappa_{\text{ex}} \langle \hat{c} \rangle, \quad (13)$$

with the external loss rate $\kappa_{\text{ex}} = \eta\kappa$. When the coupling parameter $\eta \ll 1$, the cavity is undercoupling, and when $\eta \simeq 1$, the cavity is overcoupled [4]. Experimentally, η can be continuously adjusted [49,50].

Here, we concentrate on the component of the output field oscillating at the probe frequency. To study the phase-dependent optical response properties for the probe field, we define the corresponding quadratures of the field $\varepsilon_T = \kappa_{\text{ex}} \langle \delta \hat{c} \rangle / \varepsilon_p$. The transmission coefficient and power transmission coefficient can be further defined as $T = -1 + \varepsilon_T$ and $T = |T|^2$, respectively. At weak cavity-waveguide coupling $\eta \ll 1$, $|T| \simeq 1 - \text{Re}(\varepsilon_T)$, $\arg(T) \simeq -\text{Im}(\varepsilon_T)$. Thus, similar to atomic physics, we can use the real and imaginary parts of ε_T to represent absorptive and dispersive behavior of the probe field. In the following, the ratio between $|\varepsilon_a|$ and $|\varepsilon_p|$ is defined as $y = |\varepsilon_a/\varepsilon_p|$.

III. PHASE-DEPENDENT OPTICAL RESPONSE PROPERTIES FOR THE PROBE FIELD

A. GWI-like absorption spectra

Here we assume $|G| > \sqrt{\kappa\gamma_m}/2$, i.e., the cooperativity $C = 4|G|^2/(\kappa\gamma_m) > 1$. In this regime, one can obtain typical OMIT or Autler-Townes splitting spectra if only the control and the probe fields are applied. But if an additional driving field is applied on the mechanical resonator, the interference between the OMIT process and the phonon-photon parametric process [represented by the first and the second terms in Eq. (12), respectively] can lead to the expected phase-dependent absorption spectra. In Figs. 2(a)–2(d), we plot absorption $\text{Re}(\varepsilon_T)$, dispersion $\text{Im}(\varepsilon_T)$, and power transmission coefficient T versus Δ' for different relative phase Φ . For simplicity, we have assumed the ratio of amplitude between the two weak drivings $y = |\varepsilon_a/\varepsilon_p| = 1$. When $\Phi = 0$, the interference of the two terms in Eq. (12) results in absorption and anomalous dispersion around $\Delta' = 0$. When $\Phi = \pi/2$, we can get asymmetric gain spectra with transparency point at $\Delta' \simeq 0$ and absorption and amplification appear in the red- and blue-detuned regions, respectively. The nature of dispersion is normal in the transparency and amplification regions where quantum interferences are prominent. When $\Phi = \pi$, a remarkable probe gain can be established between

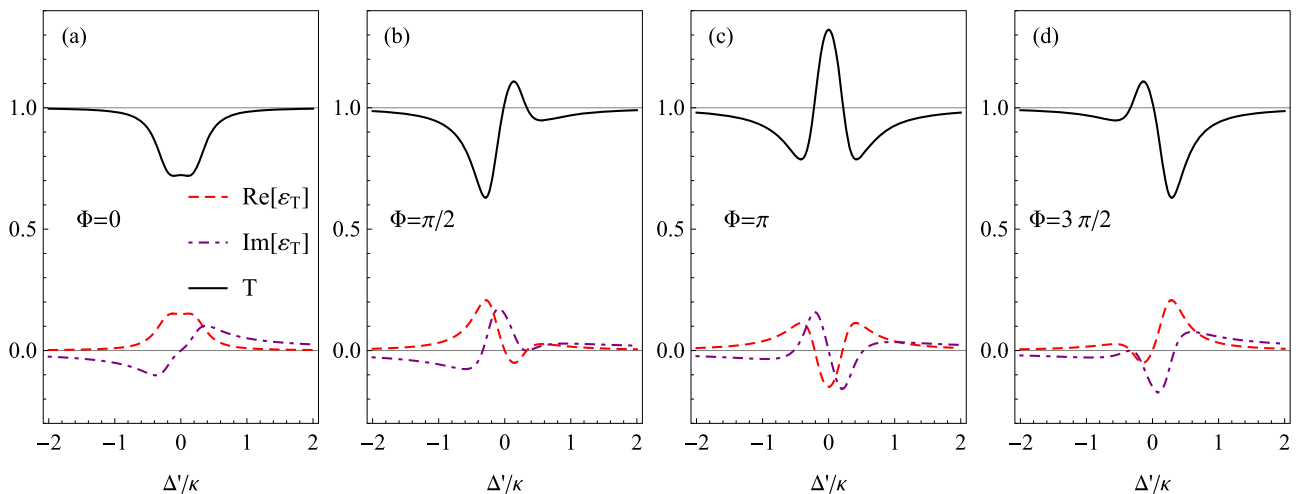


FIG. 2. (Color online) Phase-dependent absorption (dashed line), dispersion (dash-dotted line), and power transmission coefficient (solid line) versus Δ' for different phase factor: (a) $\Phi = 0$; (b) $\Phi = \pi/2$; (c) $\Phi = \pi$; (d) $\Phi = 3\pi/2$. Other parameters are $|G| = \kappa/3$, $\omega_m = 10\kappa$, $\gamma_m = \kappa/1000$, $\eta = 0.05$, $y = 1$.

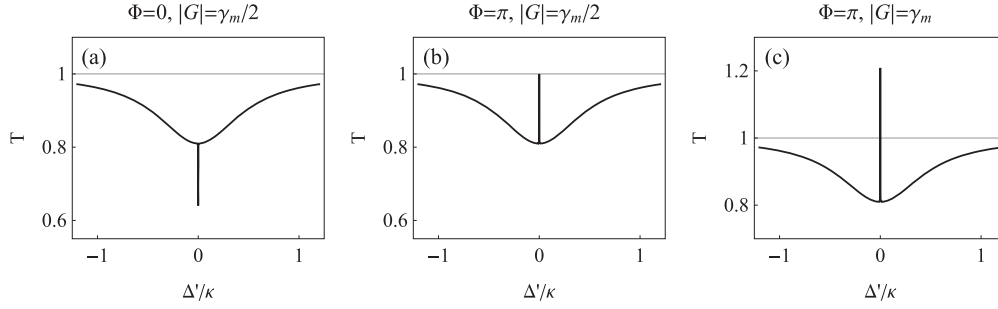


FIG. 3. Phase-dependent power transmission coefficient versus Δ' with $\Phi = 0$, $|G| = \gamma_m/2$ in (a); $\Phi = \pi$, $|G| = \gamma_m/2$ in (b); $\Phi = \pi$, $|G| = \gamma_m$ in (c). Other parameters are the same as in Fig. 2.

two Autler-Townes absorption peaks, with the maximum gain point being located at $\Delta' = 0$. The curve of $\text{Im}(\varepsilon_T)$ exhibits normal dispersive behavior in the amplification regime. When $\Phi = 3\pi/2$, we attain the mirror image of the $\Phi = \pi/2$ absorption curve.

Note that Figs. 2(a)–2(d) exhibit the similar type of phase-dependent GWI absorption spectra as those in Δ -type superconducting artificial atoms [43,44]. But there also exist some differences between them. Specifically, a Δ -type artificial atom is a three-level system, and one can easily check that when such an atom is driven by three coherent fields (i.e., a strong control, a weak probe, and an additional weak auxiliary field, respectively), the populations of the two levels related to the probe transition are inversionless [43,44]. While an optomechanical cavity is a system with an infinite number of energy levels $|N_c, N_m\rangle$ [$N_c(N_m)$ denotes the number of photons (phonons)], the probe field couples all the transitions $|N_c, N_m\rangle \leftrightarrow |N_c + 1, N_m\rangle$ [see Fig. 1(b)], and the population-inversionless condition between these pairs of states is not necessarily satisfied. Thus we term the spectra in Fig. 2 as *GW-like absorption spectra*.

B. Weak control field regime: OMIA and EIT-like spectra

When $|G| \ll \sqrt{\kappa\gamma_m}/2$, i.e., the cooperativity $C \ll 1$, the expectation value of the fluctuation operator $\delta\hat{c}$ can be approximately written as

$$\langle \delta\hat{c} \rangle = e^{i\phi_p} \left[\frac{|\varepsilon_p|}{\frac{\kappa}{2} - i\Delta'} + \frac{2|\varepsilon_a||G|e^{i\Phi}}{\kappa\left(\frac{\gamma_m}{2} - i\Delta'\right)} \right]. \quad (14)$$

Clearly, the first term shows that in this parameter regime, the OMIT effect vanishes, the probe absorption spectrum will exhibit the usual Lorentz line shape with width κ in the absence of the driving field ε_a . However, in our case, due to the existence of ε_a , the photons generated by the phonon-photon parametric process can interfere (depending on the phase factor Φ) with the photons directly excited by the probe beam. The absorptive behavior of the probe field can be represented by the real part of the quadrature of the field,

$$\text{Re}(\varepsilon_T) = \frac{\kappa_{\text{ex}}}{2} \left[\frac{\kappa}{\frac{\kappa^2}{4} + \Delta'^2} + \frac{2|G|(\gamma_m \cos \Phi - 2\Delta' \sin \Phi)}{\kappa\left(\frac{\gamma_m^2}{4} + \Delta'^2\right)} \right], \quad (15)$$

which depends on the phase factor Φ . Note that without loss of generality, we have let the ratio of amplitude between the two weak drivings equals to one (i.e., $y = 1$). Typically, when $\Phi = 0$ or $\Phi = \pi$, we have

$$\text{Re}(\varepsilon_T) = \frac{\kappa_{\text{ex}}}{2} \left[\frac{\kappa}{\frac{\kappa^2}{4} + \Delta'^2} \pm \frac{2|G|\gamma_m}{\kappa\left(\frac{\gamma_m^2}{4} + \Delta'^2\right)} \right]. \quad (16)$$

Here, the sign “+” and “−” correspond to relative phase $\Phi = 0$ and $\Phi = \pi$, respectively. Equation (16) is composed of a sum of two Lorentzians with width κ and γ_m , respectively. In addition, when $\Phi = 0(\pi)$, constructive (destructive) interference appears. In Figs. 3(a)–3(c) we plot power transmission coefficient $T = 1 - 2\text{Re}(\varepsilon_T)$ curves to display these kinds of spectral structures resulting from phase-dependent constructive or destructive interference effects.

Specifically, when $\Phi = 0$, constructive interference occurs at $\Delta' = 0$, resulting in a typical OMIA spectrum with a very sharp absorption feature around the resonant point, as shown in Fig. 3(a). Note that in optomechanical setups, a similar OMIA spectrum for a probe field can also be obtained by placing a pump blue-detuned at a mechanical frequency away from cavity [13,24]. Also, another version of OMIA was predicted in a driving double-cavity configuration, where the absorption peak is established in the OMIT window [25]. When $\Phi = \pi$, destructive interference occurs, thus a transparency or an amplification window can appear at the resonance point, depending on the value of $|G|$. According to Eq. (16), when $|G| = \gamma_m/2$, the absorption $\text{Re}(\varepsilon_T) = 0$ at resonant point. In this case, an EIT-like power transmission curve can be obtained with the value of T at the transparency dip being exactly one, as shown in Fig. 3(b). When $|G| > \gamma_m/2$, $\text{Re}(\varepsilon_T) < 0$ (i.e., $T > 0$), a gain dip can be established in the vicinity of the cavity resonant point, as shown in Fig. 3(c).

Let us now make comparisons between the EIT-like phenomenon shown in Fig. 3(b), and the standard OMIT phenomenon [8–14]. In both cases, the coherent oscillation of the mechanical resonator induces sidebands on the cavity field. Thus photons with frequency ω_p is generated and interfere destructively with the probe beam, resulting in a sharp transparency window splitting the probe absorption peak. However, the coherent oscillation of the mechanical resonator is attributed to a different mechanism in these two cases. In the standard OMIT phenomenon, the mechanical resonator is driven by a time-varying radiation pressure force induced by the beat of the probe laser and the control laser, and oscillates

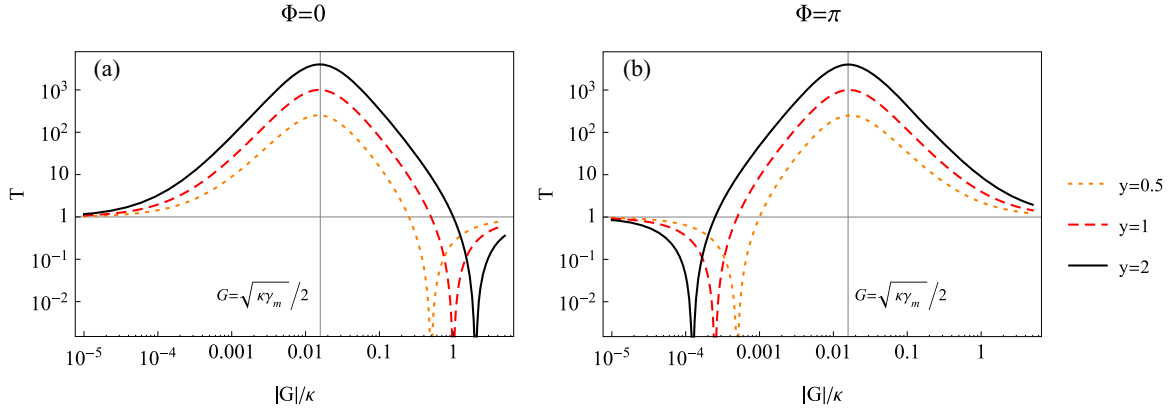


FIG. 4. (Color online) The power transmission coefficient for the probe as function of $|G|$ for various y , is plotted with $\Phi = 0$ in (a) and $\Phi = \pi$ in (b). In all cases, the cavity-waveguide coupling parameter is $\eta = 1$. Other parameters are the same as in Fig. 2.

coherently. To manifest this effect, a relatively large effective optomechanical coupling constant with $|G| \gtrsim \sqrt{\kappa\gamma_m}/2$ (i.e., $C \gtrsim 1$) is required. While in the present EIT-like case, $|G| = \gamma_m/2 \ll \sqrt{\kappa\gamma_m}/2$, the usual OMIT effect already vanishes, but the mechanical resonator is still directly driven by the external driving field with amplitude ε_a and oscillates coherently. Thus the EIT-like effect may provide an alternative way to control photon propagation even if the control field is too weak to produce the usual OMIT phenomenon. Note that in a recent experiment on coherent signal transfer between microwave and optical fields, this type of phenomenon has been used to demonstrate coherent interactions between microwave, mechanical, and optical modes [38].

C. Amplification and perfect absorption for the probe beam

Usually, an amplifier based on the optomechanical setup is realized by pumping the optomechanical cavity by a blue-detuned control field [13,14,26]. Our proposal shows that a red-detuned control field associating with an auxiliary driving applied to the mechanical resonator can also realize probe amplification. In previous subsections, to get power transmission spectra analogous to those investigated in atomic gases (such as EIA, GWI), we have taken the coupling parameter $\eta \ll 1$, and have shown a gain dip around $\Delta' = 0$ when $\Phi = \pi$ [see Figs. 2(c) and 3(c)]. Here, to obtain a remarkable amplification for a resonantly injected probe, we take $\eta = 1$ (i.e., the cavity is over-coupled) and Φ is equal to either 0 or π . Substituting Eq. (12) into relation $T = |-1 + \varepsilon_T|^2$ and letting $\Delta' = 0$, we get the power transmission coefficient at the resonant point as a function of $|G|$:

$$T = \left(\frac{\frac{\kappa\gamma_m}{4} \pm y\kappa|G| - |G|^2}{\frac{\kappa\gamma_m}{4} + |G|^2} \right)^2. \quad (17)$$

Here, the sign “+” and “−” correspond to relative phase $\Phi = 0$ and $\Phi = \pi$, respectively. From Eq. (17), we can find that a resonant probe can be effectively amplified, the main results can be summarized as follows: (i) when $\Phi = 0$, under the condition $\kappa \ll \gamma_m$, as is often the case in cavity optomechanics, the amplification region (with $T > 1$) is approximately $|G| < y\kappa/2$; (ii) when $\Phi = \pi$, the amplification region is approximately $|G| > \gamma_m/(2y)$; (iii) in both $\Phi = 0$ and $\Phi = \pi$

cases, when $|G| \simeq \sqrt{\kappa\gamma_m}/2$ (i.e., the cooperativity $C \simeq 1$), for different ratio y between the amplitudes of the two weak fields, $dT/d|G| = 0$, $d^2T/d|G|^2 < 0$, the output power for the field at probe frequency ω_p achieves maximum with power transmission coefficient $T_{\max} \simeq y^2\kappa/\gamma_m$. Figures 4(a) and 4(b) show the amplitude of the output power from the cavity as a function of $|G|$ in these cases.

Physically, the extra energy of the amplified probe is due to the contribution of the phonon-photon parametric process described by the second term in Eq. (12), whose strength is dependent on the coherent photons (excited by ε_c) in the cavity and phonons (excited by ε_a) in the mechanical resonator. On one hand, for a given probe, increasing y (by increasing $|\varepsilon_a|$) can excite more phonons in the mechanical resonator, leading to a more remarkable amplification, as shown in Figs. 4(a) and 4(b). On the other hand, an increasing $|G|$ (by increasing $|\varepsilon_c|$) can produce more photons in the cavity but at the same time lower the phonon numbers in the mechanical resonator for the existence of sideband cooling effect. The first process contributes positively and the second one negatively to the phonon-photon parametric process, resulting in maximal amplification appearing at $|G| \simeq \sqrt{\kappa\gamma_m}/2$, as shown in Figs. 4(a) and 4(b). Note that at the maximal amplification point, the modulus of the expectation value $|\langle \delta\hat{\varepsilon} \rangle|$ may be very large, to ensure the validity of the linearize theory, $|\langle \delta\hat{\varepsilon} \rangle|/c_s \ll 1$ should be satisfied. Using this relation, we can estimate that the condition $\sqrt{T_{\max}} |\varepsilon_p/\varepsilon_c| \ll 1$ (i.e., the probe magnitude after amplification must have a lower value than that of the control field) must be satisfied to ensure the validity of the linear-regime analysis.

In addition, Eq. (17) shows that when $\Phi = 0$ and $|G| \simeq y\kappa$, or $\Phi = \pi$ and $|G| \simeq \gamma_m/(4y)$, the power transmission coefficient for a resonant injected probe beam is zero. This means that the probe can be totally absorbed. These results can be clearly seen in Figs. 4(a) and 4(b). It is known that for the over-coupled case $\eta = 1$, if a single probe laser drives the cavity, the output probe beam will leave the cavity without any absorption [3]. However, in our case, because a control field ε_c and an auxiliary driving field ε_a are applied, destructive interference can lead to zero output for the probe field. Thus, the device may be used as a quantum switch to control the photon propagation in the future quantum network. We note that similar perfect absorption phenomena also exist

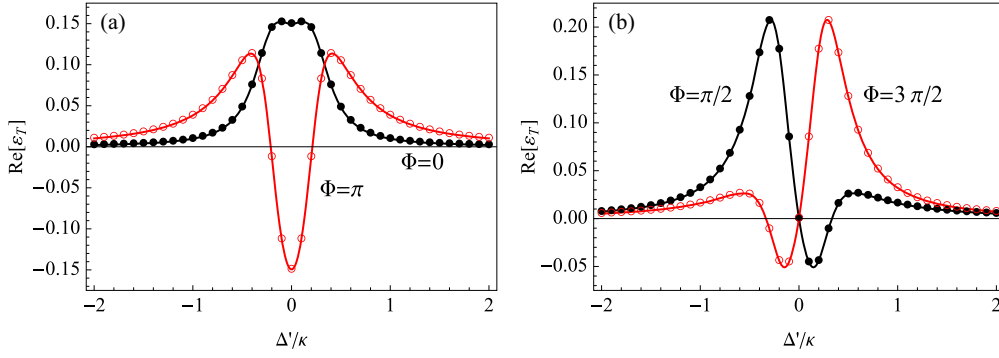


FIG. 5. (Color online) Comparison between the numerical (dots and circles) and the analytical (solid curves) results of the phase-dependent absorption spectra with (a) $\Phi = 0, \pi$; (b) $\Phi = \pi/2, 3\pi/2$. The average thermal phonon number $N_{\text{th}} = 10$. The coupling strength $|G| = \kappa/3$. The probe amplitude $|\varepsilon_p| = \kappa/30$. Other parameters are the same as in Fig. 2.

in two-side driving resonator-in-middle-type optomechanical systems [51,52].

D. Numerical results

In this part, to verify the above phase-dependent spectral structure obtained analytically, we give numerical results by solving the master equation. The quantum Langevin Eqs. (8) and (9) correspond to an effective Hamiltonian,

$$\begin{aligned} \hat{H}_{\text{eff}} = & -\hbar\Delta'(\delta\hat{c}^\dagger\delta\hat{c} + \delta\hat{b}^\dagger\delta\hat{b}) - (\hbar G\delta\hat{c}^\dagger\delta\hat{b} + \hbar G^*\delta\hat{c}\delta\hat{b}^\dagger) \\ & + (i\hbar\varepsilon_p\delta\hat{c}^\dagger + i\hbar\varepsilon_a\delta\hat{b}^\dagger + \text{H.c.}), \end{aligned} \quad (18)$$

with beam-splitter-like interaction. Based on this Hamiltonian, we can get the quantum master equation,

$$\begin{aligned} \dot{\hat{\rho}} = & \frac{1}{i\hbar}[\hat{H}_{\text{eff}}, \hat{\rho}] + \kappa\mathcal{D}[\delta\hat{c}]\hat{\rho} + \gamma_m(N_{\text{th}} + 1)\mathcal{D}[\delta\hat{b}]\hat{\rho} \\ & + \gamma_m N_{\text{th}}\mathcal{D}[\delta\hat{b}^\dagger]\hat{\rho}, \end{aligned} \quad (19)$$

describing the dynamics of the system, where $\hat{\rho}$ denotes the density matrix of the system, $\mathcal{D}[\hat{o}]\hat{\rho} = \hat{o}\hat{\rho}\hat{o}^\dagger - (\hat{o}^\dagger\hat{o}\hat{\rho} + \hat{\rho}\hat{o}^\dagger\hat{o})/2$ ($\hat{o} = \delta\hat{c}, \delta\hat{b}, \delta\hat{b}^\dagger$) is the standard dissipator in the Lindblad form, and N_{th} is the average thermal phonon number of the mechanical resonator. For a nanomechanical resonator with frequency $2\pi \times 10$ MHz, under typical environment with temperature (30 mK) in present experiments [26], the thermal phonon number N_{th} is about 10. Figure 5 gives both the numerical and analytical results of the phase-dependent probe absorption spectra. Without loss of generality, we only take the GWI-like case discussed in Sec. III A as an example. We can see that the analytical results are in good agreement with the numerical calculations.

IV. CONCLUSIONS AND DISCUSSIONS

In summary, we have explored an optomechanical system under the EIT condition with the mechanical resonator being

driven by an auxiliary coherent field. We find that the response of the driven optomechanical system to the weak probe field depends on the total phase of three classical fields. Because an additional driving field is applied to the mechanical resonator, the system will exhibit more complex quantum interference phenomena. Specifically, when the cooperativity $C = 4|G|^2/(\kappa\gamma_m) > 1$ is satisfied, we can get GWI-like spectra similar to those predicted in superconducting artificial atoms. When the cooperativity $C \ll 1$, our proposal provides a way to obtain OMIA and EIT-like spectra. When the cooperativity $C \simeq 1$, we can get remarkable amplification for the probe beam by adjusting the phase and amplitude of the coherent driving field applied on the mechanical resonator. We also give numerical results including thermal decoherence by solving the master equation. The numerical results are in good agreement with the analytical ones. Experimentally, there are various ways to coherently drive a micro- or nanoscale mechanical resonator [38–40]. This kind of optomechanical setups may be used to switch or amplify probe signals in the future quantum networks.

ACKNOWLEDGMENTS

We thank Xiao-Bo Yan and Wei Nie for useful discussions. W.Z.J. is supported by the NSFC under Grants No. 11347001 and No. 11404269, and the Fundamental Research Funds for the Central Universities under Grant No. 2682014RC21. L.F.W. is supported by the NSFC under Grants No. 11174373, No. U1330201, and No. 91321104. Y.X.L. is supported by the NSFC under Grants No. 61025022 and No. 61328502, the National Basic Research Program of China 973 Program under Grant No. 2014CB921401, the Tsinghua University Initiative Scientific Research Program, and the Tsinghua National Laboratory for Information Science and Technology (TNList) Cross-discipline Foundation. It is also supported by NSFC under Grant No. 11174027.

- [1] T. J. Kippenberg and K. J. Vahala, *Science* **321**, 1172 (2008).
 [2] F. Marquardt and S. M. Girvin, *Physics* **2**, 40 (2009).
 [3] M. Aspelmeyer, P. Meystre, and K. Schwab, *Phys. Today* **65**, 29 (2012).

- [4] M. Aspelmeyer, T. J. Kippenberg, and F. Marquardt, *Rev. Mod. Phys.* **86**, 1391 (2014).
 [5] S. E. Harris, J. E. Field, and A. Imamoglu, *Phys. Rev. Lett.* **64**, 1107 (1990).

- [6] S. E. Harris, *Phys. Today* **50**, 36 (1997).
- [7] M. Fleischhauer, A. Imamoglu, and J. P. Marangos, *Rev. Mod. Phys.* **77**, 633 (2005).
- [8] G. S. Agarwal and S. Huang, *Phys. Rev. A* **81**, 041803 (2010).
- [9] S. Huang and G. S. Agarwal, *Phys. Rev. A* **83**, 023823 (2011).
- [10] S. Huang and G. S. Agarwal, *Phys. Rev. A* **83**, 043826 (2011).
- [11] S. Weis, R. Rivière, S. Deléglise, E. Gavartin, O. Arcizet, A. Schliesser, and T. J. Kippenberg, *Science* **330**, 1520 (2010).
- [12] J. D. Teufel, D. Li, M. S. Allman, K. Cicak, A. J. Sirois, J. D. Whittaker, and R. W. Simmonds, *Nature (London)* **471**, 204 (2011).
- [13] A. H. Safavi-Naeini, T. P. M. Alegre, J. Chan, M. Eichenfield, M. Winger, Q. Lin, J. T. Hill, D. E. Chang, and O. Painter, *Nature (London)* **472**, 69 (2011).
- [14] M. Karuza, C. Biancofiore, M. Bawaj, C. Molinelli, M. Galassi, R. Natali, P. Tombesi, G. Di Giuseppe, and D. Vitali, *Phys. Rev. A* **88**, 013804 (2013).
- [15] X. Zhou, F. Hocke, A. Schliesser, A. Marx, H. Huebl, R. Gross, and T. J. Kippenberg, *Nat. Phys.* **9**, 179 (2013).
- [16] D. E. Chang, A. H. Safavi-Naeini, M. Hafezi, and O. Painter, *New J. Phys.* **13**, 023003 (2011).
- [17] H. Xiong, L.-G. Si, A.-S. Zheng, X. Yang, and Y. Wu, *Phys. Rev. A* **86**, 013815 (2012).
- [18] A. Kronwald and F. Marquardt, *Phys. Rev. Lett.* **111**, 133601 (2013).
- [19] K. Børkje, A. Nunnenkamp, J. D. Teufel, and S. M. Girvin, *Phys. Rev. Lett.* **111**, 053603 (2013).
- [20] M.-A. Lemonde, N. Didier, and A. A. Clerk, *Phys. Rev. Lett.* **111**, 053602 (2013).
- [21] A. Lezama, S. Barreiro, and A. M. Akulshin, *Phys. Rev. A* **59**, 4732 (1999); A. M. Akulshin, S. Barreiro, and A. Lezama, *ibid.* **57**, 2996 (1998); A. Lipsich, S. Barreiro, A. M. Akulshin, and A. Lezama, *ibid.* **61**, 053803 (2000).
- [22] A. V. Taichenachev, A. M. Tumaikin, and V. I. Yudin, *Phys. Rev. A* **61**, 011802 (1999).
- [23] H. Ian, Y.-X. Liu, and F. Nori, *Phys. Rev. A* **81**, 063823 (2010).
- [24] F. Hocke, X. Zhou, A. Schliesser, T. J. Kippenberg, H. Huebl, and R. Gross, *New J. Phys.* **14**, 123037 (2012).
- [25] K. Qu and G. S. Agarwal, *Phys. Rev. A* **87**, 031802 (2013).
- [26] F. Massel, T. T. Heikkilä, J.-M. Pirkkalainen, S. U. Cho, H. Saloniemi, P. J. Hakonen, and M. A. Sillanpää, *Nature (London)* **480**, 351 (2011).
- [27] A. Metelmann and A. A. Clerk, *Phys. Rev. Lett.* **112**, 133904 (2014).
- [28] A. Nunnenkamp, V. Sudhir, A. K. Feofanov, A. Roulet, and T. J. Kippenberg, *Phys. Rev. Lett.* **113**, 023604 (2014).
- [29] M. O. Scully, S. Y. Zhu, and A. Gavrielides, *Phys. Rev. Lett.* **62**, 2813 (1989).
- [30] H. Fearn, C. Keitel, M. O. Scully, and S. Y. Zhu, *Opt. Commun.* **87**, 323 (1992).
- [31] H. Li, V. A. Sautenkov, Y. V. Rostovtsev, G. R. Welch, P. R. Hemmer, and M. O. Scully, *Phys. Rev. A* **80**, 023820 (2009).
- [32] S. Menon and G. S. Agarwal, *Phys. Rev. A* **57**, 4014 (1998).
- [33] M. O. Scully, *Phys. Rep.* **219**, 191 (1992).
- [34] M. Fleischhauer, C. H. Keitel, M. O. Scully, C. Su, B. T. Ulrich, and S. Y. Zhu, *Phys. Rev. A* **46**, 1468 (1992).
- [35] M. O. Scully, K. Wódkiewicz, M. S. Zubairy, J. Bergou, N. Lu, and J. Meyer ter Vehn, *Phys. Rev. Lett.* **60**, 1832 (1988).
- [36] M. O. Scully and M. S. Zubairy, *Quantum Optics* (Cambridge University Press, Cambridge, 1997).
- [37] J. C. Petch, C. H. Keitel, P. L. Knight, and J. P. Marangos, *Phys. Rev. A* **53**, 543 (1996).
- [38] A. D. O'Connell, M. Hofheinz, M. Ansmann, R. C. Bialczak, M. Lenander, E. Lucero, M. Neeley, D. Sank, H. Wang, M. Weides, J. Wenner, J. M. Martinis, and A. N. Cleland, *Nature (London)* **464**, 697 (2010).
- [39] J. Bochmann, A. Vainsencher, D. D. Awschalom, and A. N. Cleland, *Nat. Phys.* **9**, 712 (2013).
- [40] Y.-X. Liu, A. Miranowicz, Y. B. Gao, J. Bajer, C. P. Sun, and F. Nori, *Phys. Rev. A* **82**, 032101 (2010).
- [41] D. V. Kosachiov, B. G. Matisov, and Yu. V. Rozhdestvensky, *Opt. Commun.* **85**, 209 (1991); *J. Phys. B* **25**, 2473 (1992).
- [42] Y.-X. Liu, J. Q. You, L. F. Wei, C. P. Sun, and F. Nori, *Phys. Rev. Lett.* **95**, 087001 (2005).
- [43] W. Z. Jia and L. F. Wei, *Phys. Rev. A* **82**, 013808 (2010).
- [44] J. Joo, J. Bourassa, A. Blais, and B. C. Sanders, *Phys. Rev. Lett.* **105**, 073601 (2010).
- [45] W. Z. Jia, L. F. Wei, and Z. D. Wang, *Phys. Rev. A* **83**, 023811 (2011).
- [46] P. Kraál and M. Shapiro, *Phys. Rev. Lett.* **87**, 183002 (2001); P. Kraál, I. Thanopoulos, M. Shapiro, and D. Cohen, *ibid.* **90**, 033001 (2003).
- [47] Y. Li, C. Bruder, and C. P. Sun, *Phys. Rev. Lett.* **99**, 130403 (2007).
- [48] D. F. Walls and G. J. Milburn, *Quantum Optics* (Springer-Verlag, Berlin, 1994).
- [49] M. Cai, O. Painter, and K. J. Vahala, *Phys. Rev. Lett.* **85**, 74 (2000).
- [50] S. M. Spillane, T. J. Kippenberg, O. J. Painter, and K. J. Vahala, *Phys. Rev. Lett.* **91**, 043902 (2003).
- [51] G. S. Agarwal and S. Huang, *New J. Phys.* **16**, 033023 (2014).
- [52] X. B. Yan, C. L. Cui, K. H. Gu, X. D. Tian, C. B. Fu, and J. H. Wu, *Opt. Express* **22**, 4886 (2014).